Influence of composition, many-body effects, spin-orbit coupling, and disorder on magnetism of Co-Pt solid-state systems

O. Šipr,[1,*] J. Minár,[2] S. Mankovsky,[2] and H. Ebert[2,†]
[1]*Institute of Physics of the ASCR v. v. i., Cukrovarnická 10, CZ-162 53 Prague, Czech Republic*
[2]*Department Chemie und Biochemie, Universität München, Butenandtstrasse 5-13, D-81377 München, Germany*
(Received 10 July 2008; revised manuscript received 4 September 2008; published 3 October 2008)

Systematic trends in the magnetism of Co-Pt solid-state systems are explored by studying the effects of composition, electron correlations, spin-orbit coupling (SOC), and long-range order. *Ab initio* fully relativistic calculations were performed for bulk Co, a substitutional Pt impurity in Co, Co_3Pt, CoPt, $CoPt_3$, and a substitutional Co impurity in Pt. Many-body effects beyond the local spin-density approximation (LSDA) were included via the dynamical mean-field theory (DMFT); a comparison with results based on the Brooks orbital-polarization (OP) scheme was also made. The disorder was treated within the coherent-potential approximation. We found that while the spin magnetic moments μ_{spin} at the Co atoms monotonously increase with increasing Pt concentration, the orbital magnetic moments μ_{orb} do not follow the trend of μ_{spin}. Magnetic moments μ_{spin} and μ_{orb} at Pt atoms do not depend on Pt concentration monotonously. Most of these trends can be understood in terms of hybridization and site-dependent SOC. The OP scheme of Brooks corrects the deficiencies of a pure LSDA only if the Pt concentration is low. The LSDA+DMFT scheme provides μ_{orb}/μ_{spin} ratios for Co atoms which agree with experiment even for high Pt content. Introducing disorder leads to an enhancement of μ_{spin} at Co atoms and to a suppression of μ_{spin} at Pt atoms. The μ_{orb} at Co atoms does not exhibit any systematic dependence on the degree of order, while μ_{orb} at Pt atoms decreases with increasing disorder for all Pt concentrations.

DOI: 10.1103/PhysRevB.78.144403 PACS number(s): 75.50.Cc, 75.10.Lp, 71.15.Rf

I. INTRODUCTION

Films, multilayers, and nanoparticles of Co and Pt represent an important class of new materials. As reference for such systems, one can employ bulk Co-Pt compounds which can be prepared for a wide range of compositions, in both ordered and disordered phases. Research on bulk Co-Pt alloys offers an opportunity to observe trends of magnetic properties with composition and with the degree of order and also to test the applicability of various computational procedures and approximations. Therefore, we focus in this work on ordered and disordered Co_3Pt, CoPt, and $CoPt_3$ and, additionally, on bulk hcp Co metal, on a Co impurity in a bulk Pt host, and on a Pt impurity in a bulk Co host. In that way, we cover the whole range of Co-Pt compositions. Our aim is to understand the trends of magnetism of Co-Pt systems in simple intuitive terms so that it would be possible to foresee what properties one could expect in various systems prepared from Co and Pt. We also want to connect the theoretical results with experiment, because the applicability of various computational schemes can be assessed properly only if well-defined systems—such as those we want to focus on—are involved.

A lot of research dealt with Co-Pt systems in the past. However, most of the theoretical results were acquired in studies devoted to one system at a time. Because different studies often relied on different methods, one cannot simply merge all the partial data to obtain a complete picture of the complex Co-Pt manifold. Only relatively few studies dealt with more than one Co-Pt system simultaneously;[1–7] most of them were nonrelativistic. To our knowledge no fully relativistic calculations were performed for Co impurities embedded in Pt or for Pt impurities embedded in Co. The studies performed so far indicate that the spin magnetic moment μ_{spin} at Co should increase when going from Co_3Pt to CoPt. For transitions from CoPt to $CoPt_3$, studies based on the full-potential linearized augmented plane-wave (FLAPW) or full-potential linear muffin-tin orbital (FP-LMTO) methods[2,6] suggest an increase in μ_{spin} at Co, while studies based on LMTO or Korringa-Kohn-Rostoker atomic sphere approximation (KKR-ASA) predict a decrease in μ_{spin}.[1,3,7] For μ_{spin} at Pt atoms, most studies suggest a slight increase when going from Co_3Pt to CoPt followed by a sharp drop when going from CoPt to $CoPt_3$. As concerns the orbital magnetic moment μ_{orb}, only pairs of Co-Pt systems were compared in the past: It was found that μ_{orb} at Co as well as at Pt atoms drops when going from CoPt to $CoPt_3$ (Ref. 6) and when going from Co_3Pt to $CoPt_3$.[4] Influence of many-body effects beyond the local spin-density approximation (LSDA) was tested on CoPt only. It was found that μ_{orb} at the Co atom increases when applying the Brooks orbital-polarization (OP) scheme[8,9] or the corrected random-phase approximation[10] or the LSDA+U method.[11]

The transition from ordered Co-Pt compounds to substitutionally disordered alloys was investigated via nonrelativistic calculations using the coherent-potential approximation (CPA) method and using the augmented space recursion (ASR) method.[7] The CPA calculations suggest that introducing disorder leads to an increase in μ_{spin} at the Co atoms for all compositions, while μ_{spin} at the Pt atoms should decrease for Co_3Pt and CoPt and increase for $CoPt_3$. On the other hand, the ASR calculations lead to a decrease in μ_{spin} at both the Co and the Pt atoms, for all compositions. As concerns relativistic investigations of disordered Co-Pt alloys, average magnetic moments and atom-resolved spin magnetic moments[12,13] and orbital magnetic moments at Co atoms[14] have been studied so far.

Experimental studies of Co-Pt systems can be divided into three categories. First, there are relatively old neutron-diffraction data for CoPt and $CoPt_3$ from which local moments on Co and Pt atoms were deduced.[15–17] The agreement of recent theoretical results with these atom-specific experimental data is usually not very good. Second, magnetization measurements of Co-Pt systems are available which provide average magnetic moments per atom for both ordered and disordered Co-Pt alloys (and also for a Co impurity in Pt).[18–21] For this type of data, the agreement between theory and experiment is usually quite good. Finally, atom-specific μ_{spin} and μ_{orb} and, more reliably, μ_{orb}/μ_{spin} ratios were extracted from x-ray magnetic circular dichroism (XMCD) measurements for CoPt (Refs. 22 and 23) and $CoPt_3$.[24–26] The μ_{orb}/μ_{spin} ratios obtained in this way are usually larger than those provided by theory.

In this work, we calculate spin and orbital magnetic moments for the whole range of compositions of ordered and disordered Co-Pt systems via the fully relativistic spin-polarized Korringa-Kohn-Rostoker method. Most calculations are done in the full-potential mode. Many-body effects beyond the LSDA are included via a fully self-consistent LSDA plus dynamical mean-field theory (DMFT) formalism and compared to results obtained via the more heuristic OP scheme of Brooks. The disorder is treated by the CPA method.

All the systems are treated within the same computational framework (multiple scattering) and the results for different systems are thus directly comparable. This makes it possible for us to investigate systematically the dependence of magnetic moments on the composition of the Co-Pt systems and on the degree of the long-range order. By including the spin-orbit coupling (SOC) selectively on certain sites only, further insight into the way μ_{orb} depends on the Co-Pt composition could be obtained.

II. METHODOLOGICAL FRAMEWORK

A. Investigated systems

The series of Co-Pt systems we investigated comprises (in the order of increasing Pt concentration) bulk hcp Co, a substitutional Pt impurity in hcp Co, Co_3Pt in the $L1_2$ structure, CoPt in the $L1_0$ structure, $CoPt_3$ in the $L1_2$ structure, and a substitutional Co impurity in fcc Pt. Experimental lattice constants as given, e.g., by Kootte *et al.*[1] or Paudyal *et al.*[7] were used. For systems containing impurities, no structural relaxation was performed. The numbers of Co and Pt atoms in the nearest neighborhood of each atomic type in the ordered compounds are shown in the second and third columns of Tables I and II. The fourth and the fifth columns contain the same data for the disordered systems. (In that case, the numbers of Co and Pt atoms in the first coordination shell are determined by their concentrations.) The last columns of Tables I and II display the nearest-neighbor distances.

In some experimental studies, Co-Pt systems with a partial chemical long-range order (LRO) were considered.[16,23] This concept assumes that the binary system is formed by a weighted superposition of two sublattices, one of which has the "correct" distribution of the A and B atoms among the lattice sites (i.e., the same as for ordered systems) and the other one has this distribution reversed (i.e., the A atoms are located on sites which are normally occupied by the B atoms and vice versa). The ordering parameter S of a partially ordered system is related to the fractions u_A and u_B of sites which are correctly occupied by the A and B types, respectively.[27] For an AB compound of the $L1_0$ structure, S can be evaluated as

$$S = u_A + u_B - 1, \tag{1}$$

and for an A_3B compound of the $L1_2$ structure, one has

$$S = 3\left(u_A - \frac{3}{4}\right) + \frac{1}{3}\left(u_B - \frac{1}{4}\right). \tag{2}$$

One gets $S=1$ for an ordered compound and $S=0$ for a disordered alloy. In accordance with Eqs. (1) and (2), a partially ordered CoPt with $S=0.6$ investigated by Grange *et al.*[23] was modeled by $Co_{0.8}Pt_{0.2}Pt_{0.8}Co_{0.2}$ and a partially ordered $CoPt_3$ with $S=0.6$ investigated by Menzinger and Paoletti[16] was modeled by $Co_{0.7}Pt_{0.3}(Pt_{0.9}Co_{0.1})_3$ (see Sec. III E).

Unless explicitly stated otherwise, all the results presented here correspond to the magnetization $\boldsymbol{M}$ oriented along the [001] direction of the "parental" fcc lattice (for hcp Co, $\boldsymbol{M}$ is in the [0001] direction). This choice corresponds to the easy magnetization axis for ordered CoPt (Ref. 5) and for a Co impurity in Pt.[28] On the other hand, for ordered $CoPt_3$ and for disordered $Co_{1-x}Pt_x$, the easy magnetization axis is [111].[5,29] We keep $\boldsymbol{M}\|[001]$ for all systems in order to make comparison between different materials more straightfor-

TABLE I. Numbers of Co and Pt atoms contained in the first coordination sphere around Co atoms in ordered and disordered Co-Pt systems. The nearest-neighbor distance is shown in the last column.

	Ordered		Disordered		r_1
	Co	**Pt**	**Co**	**Pt**	(Å)
Co bulk	12	0	12	0	2.51
Co_3Pt	8	4	9	3	2.59
CoPt	4	8	6	6	2.67
$CoPt_3$	0	12	3	9	2.72
Co in Pt	0	12	0	12	2.77

TABLE II. Numbers of Co and Pt atoms contained in the first coordination sphere around Pt atoms. This table is analogous to Table I.

	Ordered		Disordered		r_1
	Co	**Pt**	**Co**	**Pt**	(Å)
Pt in Co	12	0	12	0	2.51
Co_3Pt	12	0	9	3	2.59
CoPt	8	4	6	6	2.67
$CoPt_3$	4	8	3	9	2.72
Pt bulk	0	12	0	12	2.77

ward. Apart from the special case of CoPt (cf. end of Sec. III A 1), the calculated μ_{spin} and μ_{orb} do not depend on the magnetization direction very significantly. We verified that all the systematic trends we observed would remain even if $\boldsymbol{M}$ was allowed to switch from the [001] to the [111] direction (i.e., along the easy magnetization axis in the case of $CoPt_3$ and $Co_{1-x}Pt_x$).

B. Computational scheme

The calculations were performed within the *ab initio* spin-density-functional framework, relying on the LSDA. The parametrization by Vosko *et al.*[30] of the exchange and correlation potential was used. The electronic structure was calculated in a fully relativistic mode, by solving the corresponding Dirac equation. This was achieved using the spin-polarized relativistic (SPR) multiple-scattering or KKR formalism.[31,32] The impurities were treated via the real-space embedded-cluster technique,[33,34] meaning that the electronic structure of the host atoms was allowed to adjust itself to the presence of the impurity. The embedded clusters comprised 81 or 87 atoms for the Co or Pt host, respectively. The embedded-cluster technique was employed also for calculations for bulk systems in the case that the SOC was included on a single atom only (Sec. III C).

The effective potentials were treated either in a full-potential scheme (FP) or within the ASA. For the multipole expansion of Green's function, an angular momentum cutoff of $\ell_{max}=3$ was used. The integration in the $\boldsymbol{k}$ space was performed on a regular mesh. Disordered systems were treated via the self-consistent relativistic KKR-CPA method. The numerical accuracy of our results was better than $0.005\mu_B$ for μ_{spin} and $0.002\mu_B$ for μ_{orb}.

When doing FP calculations, we divided the space into cells (Voronoi polyhedra)[35] which had equal sizes for Co and for Pt atoms. For ASA calculations of ordered Co-Pt compounds, the radii of the spheres around Co and Pt sites were chosen by requiring the ratios of the corresponding volumes to be the same as in bulk elements. In order to facilitate comparison with results for disordered systems and also in order to correct for some deficiencies of the ASA, calculations with equal radii of the spheres around Co and Pt atoms were performed as well. (For disordered alloys, the radii around all atoms in a compound were taken to be identical.)

Orbital magnetic moments are often influenced by effects that cannot be described by the LSDA. For free atoms, there exists an intra-atomic orbital-polarization effect due to electronic correlations that is responsible for maximal μ_{orb} as given by the second Hund's rule. In this work we employ a heuristic method for incorporating this effect in solids suggested by Brooks.[36] According to this scheme, an additional term proportional to the Racah parameter times the square of the orbital moment is included in the Hamiltonian.

Another way of going beyond the LSDA is to include dynamical correlation effects within the framework of the DMFT. In this work, we employed a combined LSDA+DMFT scheme, self-consistent in both the self-energy and in the charge density, as implemented within the relativistic SPR-KKR formalism.[37] As the DMFT solver, a relativistic version of the so-called spin-polarized T matrix plus fluctuation exchange (SPTF) approximation[38,39] was used. According to this scheme, the local Green's function is obtained by the corresponding site projection of the full KKR Green's function. The local Green's function is needed to obtain the bath Green's function for the Anderson impurity model via the saddle-point equation. The bath Green's function is used as an input for the SPTF scheme to calculate the local self-energy. The latter is added as an additional energy-dependent potential into the radial Dirac equation, which is solved to calculate the new full KKR Green's function. This procedure is repeated until a self-consistency in both the self-energy and the charge density is achieved. The double-counting problem (separation of the Hubbard Hamiltonian from the LSDA one) was dealt with within the around mean-field limit. The DMFT calculations have been done at $T=400$ K and we used 4096 Matsubara poles to calculate the corresponding SPTF self-energy. This scheme was successfully used before in describing magneto-optics,[40] photoemission,[41] and orbital magnetic moments[42] in $3d$ transition metals.

The self-energy within the DMFT is parametrized by the average screened Coulomb interaction U and the Hund exchange interaction J. The J parameter can be calculated directly within the LSDA and is approximately the same for all $3d$ elements; we used $J_{Co}=0.9$ eV for the Co atoms throughout our work. The parameter U is strongly affected by the metallic screening; its estimates for the $3d$ metals vary as 1–3 eV. We used $U_{Co}=2.3$ eV for the Co atoms. Chadov *et al.*[42] showed recently that this choice of U_{Co} gives the best agreement between the theory and the experiment for the orbital magnetic moments in hcp Co and in FeCo disordered alloys.

As concerns the Pt atoms, the local correlation effects are often assumed to be insignificant for noble metals. However, Shick and Mryasov[11] suggested recently in their LSDA+U study that a nonzero U on Pt is necessary to reproduce the magnetic anisotropy of FePt and CoPt. We tested three different models in this work, namely: (i) $U_{Pt}=J_{Pt}=0$, (ii) $U_{Pt}=0.5$ eV and $J_{Pt}=0.5$ eV (values similar to those of Shick and Mryasov[11]), and (iii) $U_{Pt}=2.0$ eV and $J_{Pt}=0.9$ eV (i.e., similar values as for Co).

III. RESULTS AND DISCUSSION

A. Magnetic moments within LSDA

1. Basic trends of μ_{spin} and μ_{orb}

Results of our LSDA calculations of μ_{spin} and μ_{orb} as assigned to individual atoms in a series of ordered Co-Pt systems comprising pure Co, Pt impurity in Co, Co_3Pt, CoPt, $CoPt_3$, and Co impurity in Pt are shown in Fig. 1. (The compounds are labeled by their Pt content on the horizontal axis.) For compounds with the $L1_2$ structure, atoms of the same chemical type need not be all equivalent because the presence of magnetization and of SOC lowers the symmetry. In that case, averaged values are displayed (see the second half of Sec. III C for more details).

One can see a clear trend of μ_{spin} at Co to increase with increasing Pt content. This is consistent with reduction in the

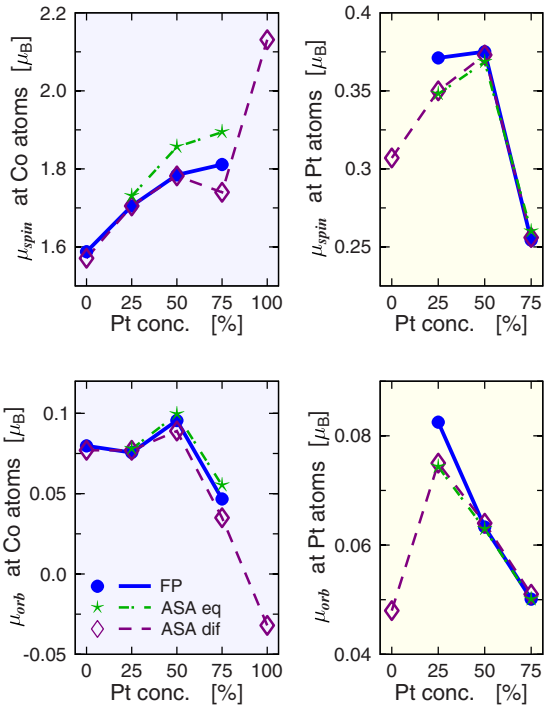

FIG. 1. (Color online) Spin (top) and orbital (bottom) magnetic moments at Co (left) and Pt atoms (right) for a series of ordered Co-Pt systems. FP results are shown as solid lines with circles. Results of ASA calculation are shown as chain lines with stars (atomic radii of Co and Pt are equal) and via broken lines with diamonds (atomic radii of Co and Pt differ). The labels on the horizontal axes show the Pt concentration in the system. Note that the Pt data for a 0% Pt concentration stand for a Pt impurity hosted in bulk Co and the Co data for a 100% Pt concentration stand for a Co impurity hosted in bulk Pt.

hybridization between Co atoms along the Co-Pt series by expanding the interatomic distances and by decreasing the number of Co neighbors (see Table I).

Local μ_{spin} at Pt atoms, on the other hand, does not vary monotonously. This can be understood by realizing that μ_{spin} induced at Pt is influenced by a competition between several trends. Namely, an increase in interatomic distances and an increase in magnetic moments at Co atoms with increasing Pt content should contribute to an increase in μ_{spin} at Pt. On the other hand, a decrease in the number of Co neighbors of Pt atoms contributes to a decrease in μ_{spin} at Pt atoms. For a more instructive view, we compare in Fig. 2 the moment μ_{spin} at Pt atoms with the product $N_{\mathrm{Co}}\mu_{\mathrm{spin}}^{(\mathrm{Co})}$ of the number N_{Co} of Co atoms in the first coordination sphere around the Pt atom with the spin magnetic moments $\mu_{\mathrm{spin}}^{(\mathrm{Co})}$ at those atoms. This product could be seen as the "total inducing strength" acting on the Pt atom. It follows from Fig. 2 that this simple picture accounts to some extent for the trend of the induced magnetism of Pt but, at the same time, it is evident that μ_{spin} at Pt is *not* just proportional to $N_{\mathrm{Co}}\mu_{\mathrm{spin}}^{(\mathrm{Co})}$.

There is an interesting difference between the weights of individual angular momentum components in μ_{spin} at the Co and at the Pt atoms. At both types of atoms, the dominant d component $\mu_{\mathrm{spin}}^{(d)}$ is always larger than the total μ_{spin} (i.e., contributions of the s and p states are antiparallel to the

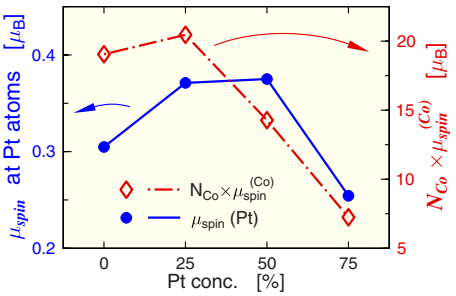

FIG. 2. (Color online) Spin magnetic moments at Pt atoms in ordered Co-Pt systems (solid line with circles, scale on the left vertical axis) compared to the sum of spin magnetic moments of all Co atoms which are nearest neighbors of the Pt atom (chain line with diamonds, scale on the right vertical axis).

contributions of the d states). However, while for Co atoms the difference between $\mu_{\mathrm{spin}}^{(d)}$ and μ_{spin} is typically less than 1%, for Pt atoms this difference is quite big—up to 20%.

For Co_3Pt, CoPt, and $CoPt_3$, our results on μ_{spin} can be compared with earlier studies of the same triad.[1,3,7] Generally, all the calculations yield very similar trends. The only exception is μ_{spin} of Co atoms in Co_3Pt as obtained by Kashyap *et al.*,[3] which is significantly lower than what all the other studies suggest. As concerns μ_{orb}, there is good agreement between our data for CoPt and $CoPt_3$ and the results of Galanakis *et al.*[6] and between our data for Co_3Pt and $CoPt_3$ and the results of Antonov *et al.*[4]

Results presented in Fig. 1 were obtained for the magnetization $\boldsymbol{M}$ in the [001] direction (parallel to the c axis). We also performed self-consistent calculations with $\boldsymbol{M}$ oriented also along the [111] direction (the easy axis of Co_3Pt and $CoPt_3$). As anticipated, no significant changes in μ_{spin} occur. The same is true also for μ_{orb} in Co_3Pt and $CoPt_3$ (the relative changes are 3% at most). This is not surprising either, as the anisotropy of cubic systems is low. An appreciable anisotropy of μ_{orb} appears only for tetragonal CoPt. μ_{orb} at Co is larger for $\boldsymbol{M}\|[001]$ (by $0.02\mu_B$) and μ_{orb} at Pt is larger for $\boldsymbol{M}\|[111]$ (by $0.01\mu_B$). These values are consistent with the anisotropies calculated for CoPt by Solovyev *et al.*,[43] Oppeneer,[44] and Ravindran *et al.*[9] Before such a comparison is made, however, one has to account for the fact that in our case the angle between the two magnetization directions is 56° (we compare the [001] and [111] directions), while in Refs. 9, 43, and 44 this angle was 90° (because in those works, the [001] and [110] directions were compared) and that the anisotropy in μ_{orb} depends on the square of the sinus of the angle.[43]

2. Comparing FP and ASA results

By relying on the ASA, one obtains that μ_{spin} at Co is smaller for $CoPt_3$ than for CoPt, i.e., reverse of the FP results. From earlier studies that employed either the FP (Refs. 2 and 6) or ASA,[1,3,7] one deduces a similar difference. To identify the reason for this, we performed another FP calculation for $CoPt_3$, this time partitioning the space not by Voronoi polyhedra but by overlapping spherical cells (as in ASA). The results were nearly the same as for ASA. Thus,

TABLE III. Magnetic moments for a Co impurity in a bulk Pt host calculated for different sizes of the embedded cluster. The first column contains the number of atoms in the cluster, the next two columns show μ_{spin} and μ_{orb} at the central Co atom, and the last two columns show the moments contained in the whole cluster. The unit is μ_B.

Number of atoms	At Co atom only		In the whole cluster	
	μ_{spin}	μ_{orb}	μ_{spin}	μ_{orb}
1	2.269	−0.013	2.269	−0.013
55	2.098	−0.029	3.393	0.207
135	2.098	−0.029	3.579	0.229
201	2.098	−0.029	3.543	0.214

the deviation of the ASA results is caused *not* by the neglect of nonspherical contributions to the potential but by an incorrect integration of the spin densities in the "interstitial region." (There is some double counting where neighboring atomic spheres overlap but there is also omission where they do not.) Indeed, one can see that the ASA results change if the atomic radii are varied (cf. the chain line and the broken line in the upper left panel of Fig. 1).

We performed FP calculations for Co and Pt impurities in the "single-site" impurity mode, in which the host affects the impurity but the feedback from the impurity to the host is neglected. The FP and ASA calculations yield practically identical results in these cases. Consequently, one can expect that ASA calculations yield correct μ_{spin} and μ_{orb} also for true embedded impurities.

The standard ASA (with radii set according to the atomic volumes of the pure elements) thus works well along the whole Co-Pt series *except* for $CoPt_3$. This failure is connected with the fact that "local" magnetic moments need not be strictly local in reality. The assignment of magnetic moments to individual sites is not unique—not even in the FP case (it depends on the sectioning of the space into cells). Thus, care must be taken about technicalities such as the sizes of the spheres or cells if one is interested in the details and, notably, if results of different studies are to be compared. Generally, the ASA should be used with caution in situations where the atomic radii of the constituting elements are remarkably different.

3. Polarization of Pt host around Co impurity

A Co impurity in Pt belongs among the "giant-magnetic-moment" diluted systems,[18] where the total magnetic moment per impurity atom highly exceeds the magnetic moment of the impurity atoms in an elemental form. This is caused by the polarization of the host. Table III shows the dependence of the calculated magnetic moments on the size of the embedded impurity cluster (i.e., on the number of atoms for which the electron structure was allowed to relax). One can see that as concerns μ_{spin} and μ_{orb} on the Co atom itself, the convergence is achieved very quickly—even the single-site impurity model (first row in Table III) yields reasonable values. In order to describe the polarization of the Pt host atoms properly, a cluster of about 100 atoms is needed.

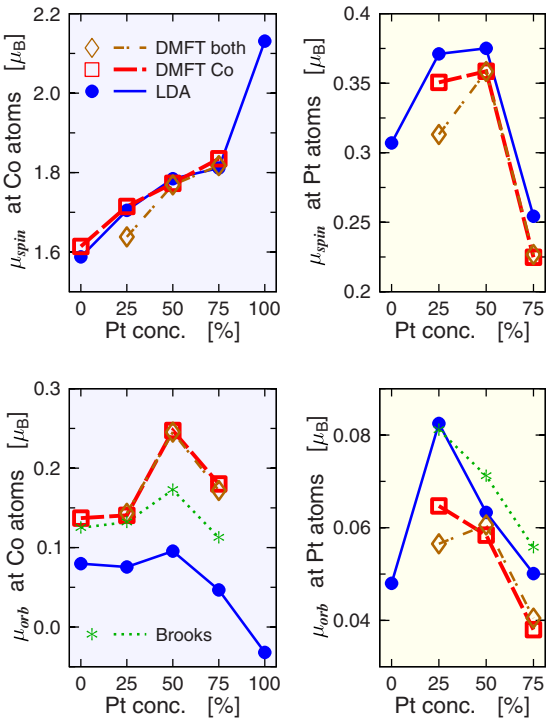

FIG. 3. (Color online) Spin (top) and orbital (bottom) magnetic moments at Co (left) and Pt atoms (right) in ordered Co-Pt systems as calculated using pure LSDA (solid lines with circles), LSDA with OP included via the Brooks scheme (dotted line with asterisks), LSDA+DMFT with U on Co atoms only (broken lines with squares), and LSDA+DMFT with U both on Co and on Pt atoms (chain lines with diamonds). Note that for the Brooks OP scheme, only μ_{orb} is shown because the corresponding μ_{spin} practically coincides with the pure LSDA results.

As concerns the moments on individual atoms, we obtained $\mu_{spin}=0.065\mu_B$ and $\mu_{orb}=0.016\mu_B$ for those Pt atoms which are nearest neighbors of the Co impurity. The extent of the polarization cloud for Pt is significantly less than for Pd, where it includes more than 1000 atoms.[45] This is consistent with the fact that the Stoner product $IN(E_F)$, where I is the Stoner exchange integral and $N(E_F)$ is the density of states at the Fermi level, is larger for Pd (0.85) than for Pt (0.59).[46]

A comparison can be made with earlier calculations made for an Au host. Frota-Pessôa[47] obtained μ_{spin} and μ_{orb} of a Co impurity in Au as $1.58\mu_B$ and $0.23\mu_B$, respectively. That means that μ_{spin} is larger if Co is embedded in Pt, while μ_{orb} is larger if Co is embedded in Au. This is consistent with the situation of a Co adatom on Pt(111) and Au(111) surfaces: One gets $\mu_{spin}=2.26\mu_B$ and $\mu_{orb}=0.64\mu_B$ for a Pt substrate and $\mu_{spin}=2.18\mu_B$ and $\mu_{orb}=1.00\mu_B$ for an Au substrate.[48]

The total (spin plus orbital) magnetic moment for Co in Pt calculated by employing the cluster of 201 atoms is $3.76\mu_B$. This is in good agreement with the experimental value of $3.6\mu_B$.[18]

B. Many-body effects

Figure 3 shows how μ_{spin} and, especially, μ_{orb} change if schemes beyond the LSDA are employed. The LSDA

TABLE IV. Magnetic moments of hcp Co obtained via different computational schemes compared with experiment. The unit is μ_B.

	μ_{tot}	μ_{spin}	μ_{orb}	μ_{orb}/μ_{spin}
LSDA	1.668	1.588	0.080	0.050
LSDA+OP	1.739	1.607	0.132	0.082
LSDA+DMFT	1.752	1.614	0.138	0.085
Expt.[a]	1.762	1.607	0.155	0.097

[a] μ_{tot} is taken from the tables (Ref. 52). The μ_{orb}/μ_{spin} ratio is taken from magnetomechanical measurements (Ref. 53).

+DMFT calculations are shown for $U_{Pt}=0$ and for $U_{Pt}=0.5$ eV (see end of Sec. II B for more details). The LSDA+DMFT results for $U_{Pt}=2.0$ eV are quite similar to the $U_{Pt}=0.5$ eV case, so we do not show them here. (The largest effect caused by increasing U_{Pt} from 0.5 to 2.0 eV is a nearly uniform increase in μ_{orb} at Pt atoms by about $0.004\mu_B$.) The LSDA and LSDA+DMFT results were obtained in the FP mode. The Brooks OP scheme results were obtained in the ASA. The data shown here are averages of the values obtained for the two choices of the atomic radii as discussed in Sec. III A 2. Only bulk Co-Pt systems are dealt with in this section—we did not apply the Brooks OP or LSDA+DMFT schemes to the impurities. Earlier calculations for Co in Ag or Au hosts suggest, nevertheless, that the LSDA+DMFT scheme could be applicable to impurities,[42] while the OP scheme of Brooks could not be applicable.[49–51]

It follows from Fig. 3 that going beyond the LSDA has only a small or even negligible effect on μ_{spin} but it has a significant effect on μ_{orb}. For the Co atoms, μ_{orb} is systematically enhanced if either the Brooks OP or DMFT corrections are added to the LSDA. The influence of either the Brooks OP or LSDA+DMFT on μ_{orb} at Pt atoms is much less significant than in the case of Co atoms. A similar trend was observed earlier for some systems of the Co-Pt series. (For bulk Co, cf. the Brooks OP calculations of Eriksson *et al.*[54] and LSDA+DMFT calculations of Chadov *et al.*[42] For CoPt, cf. the Brooks OP calculations of Daalderop *et al.*[8] and of Ravindran *et al.*,[9] random-phase-approximation calculations of Solovyev,[10] and LSDA+U calculations of Shick and Mryasov.[11]) On the other hand, extending the LSDA by incorporating the generalized gradient approximation by Galanakis *et al.*[6] did result in a systematic increase in μ_{orb} for CoPt or $CoPt_3$.

In order to see whether our way of including correlations really leads to more accurate results, we compare our results with the available experimental data in Tables IV–VI (no measurements are available for Co_3Pt). For bulk hcp Co, sufficiently reliable experimental data are available so that we can compare μ_{spin} and μ_{orb} separately. For CoPt and $CoPt_3$, the experimental values of μ_{spin} and μ_{orb} are less reliable—one has to make certain assumptions about magnetic form factors[15–17] or about x-ray-absorption matrix elements.[23,25] Therefore, for these systems we focus on the *ratios* of the orbital and spin magnetic moments, which can be extracted from XMCD measurements in a more straightforward way. The fact that the $L_{2,3}$ edge XMCD reflects only the d components of μ_{spin} and μ_{orb} poses no practical complication for Co, where the d component accounts for the total magnetic moment with an accuracy better than 5%. On the other hand, for the Pt atoms, the difference between μ_{orb}/μ_{spin} and $\mu_{orb}^{(d)}/\mu_{spin}^{(d)}$ may be up to 20% (see comment on the *sp* contributions to μ_{spin} in Sec. III A 1).

TABLE V. Quotients of the d components of μ_{orb} and μ_{spin} for Co and Pt atoms in ordered CoPt obtained via various computational schemes compared with experiment (Ref. 23). Different DMFT modes are distinguished by the value of U_{Pt}.

	U_{Pt} (eV)	Co	Pt
LSDA		0.054	0.149
LSDA+OP		0.095	0.171
LSDA+DMFT	0	0.139	0.148
LSDA+DMFT	0.5	0.138	0.153
LSDA+DMFT	2.0	0.139	0.168
Expt.		0.15	0.26

It follows from Tables IV–VI that the LSDA systematically underestimates $\mu_{orb}^{(d)}/\mu_{spin}^{(d)}$ for the Co atoms. This deficiency increases with increasing Pt content: Experimental $\mu_{orb}^{(d)}/\mu_{spin}^{(d)}$ ratio exceeds the LSDA result twice for bulk Co, three times for CoPt, and four times for $CoPt_3$. Employing the OP scheme of Brooks increases the $\mu_{orb}^{(d)}/\mu_{spin}^{(d)}$ ratio and partially compensates for the deficiency of the LSDA. This compensation is nearly complete for bulk Co but it becomes insufficient as the Pt content increases. Employing the LSDA+DMFT, on the other hand, leads to a nearly perfect reproduction of the experimental $\mu_{orb}^{(d)}/\mu_{spin}^{(d)}$ ratio at Co atoms for bulk Co, CoPt, and $CoPt_3$.

As concerns the Pt atoms, the failure of the LSDA to reproduce $\mu_{orb}^{(d)}/\mu_{spin}^{(d)}$ is not so severe as in the case of Co atoms: Theory accounts for about 60% of the experimental $\mu_{orb}^{(d)}/\mu_{spin}^{(d)}$ for CoPt and for 80% for that of $CoPt_3$ (Tables V and VI). The LSDA+DMFT does not lead to a systematic improvement over a pure LSDA in those cases. If we take $U_{Pt}=0$ (thus keeping only U_{Co} different from zero), μ_{orb} at Pt atoms decreases by 10%–20% with respect to the LSDA. If we take $U_{Pt}\neq 0$, μ_{orb} at Pt atoms increases a bit but a peculiar drop in μ_{spin} and μ_{orb} occurs for Co_3Pt (cf. Fig. 3). If we employ the Brooks OP scheme, μ_{orb} at Pt atoms increases (as well as $\mu_{orb}^{(d)}/\mu_{spin}^{(d)}$) without μ_{spin} being affected significantly. As a whole, the differences between $\mu_{orb}^{(d)}/\mu_{spin}^{(d)}$ at Pt atoms

TABLE VI. Quotients of the d components of μ_{orb} and μ_{spin} for Co and Pt atoms in ordered $CoPt_3$ obtained via different computational schemes compared with experiment (Ref. 25).

	U_{Pt} (eV)	Co	Pt
LSDA		0.026	0.176
LSDA+OP		0.065	0.200
LSDA+DMFT	0	0.099	0.153
LSDA+DMFT	0.5	0.096	0.162
LSDA+DMFT	2.0	0.090	0.186
Expt.		0.094	0.23

obtained via different computational schemes are smaller than the differences between the theory and experiment. One has to be aware, nevertheless, that the experimental $\mu_{\mathrm{orb}}^{(d)}/\mu_{\mathrm{spin}}^{(d)}$ ratio for the Pt atoms is less reliable than for the Co atoms. Namely, the XMCD sum rules[55,56] can be applied to the Pt $L_{2,3}$ edge spectra only after the contributions due to the $2p \rightarrow 5d$ transitions have been separated from the rest of the spectra. Grange *et al.*[23,25] achieved this in their studies of CoPt and $CoPt_3$ by subtracting a normalizing Au $L_{2,3}$ edge spectrum.[57] The need for such a procedure decreases the accuracy with which the magnetic moments of Pt (and of 4*d* and 5*d* metals in general) can be determined via the XMCD sum rules.

As a whole, is follows from Fig. 3 that even though the LSDA systematically underestimates μ_{orb} at Co atoms, it describes the trends of μ_{spin} and μ_{orb} with the Co-Pt composition well enough. Therefore, the following investigations of the effects of SOC and of disorder may be restricted to the LSDA.

C. Influence of spin-orbit coupling

If the spin-orbit interaction is considered as a weak perturbation, μ_{orb} at a particular site turns out to be proportional to the spin polarization at the Fermi level,[58,59]

$$\mu_{\mathrm{orb}} \sim \xi[n^{\uparrow}(E_F) - n^{\downarrow}(E_F)], \tag{3}$$

where ξ is the SOC parameter and $n^{\sigma}(E_F)$ is the local density of states (DOS) for the spin direction σ. One might thus expect that for systems where μ_{spin} is large, there would be also a large spin polarization $n^{\uparrow}(E_F) - n^{\downarrow}(E_F)$ and, consequently, a large μ_{orb} as well. The Co-Pt series defies this assumption (see Fig. 1): Indeed, μ_{orb} at Co is least for that system for which μ_{spin} is largest (i.e., for a Co impurity in Pt). This seemingly counterintuitive behavior can be understood by looking at what happens if SOC is included on some atoms only. Figure 4 shows μ_{orb} calculated (within the LSDA) if SOC is included only on a single atomic site, if SOC is included on all atoms, and if SOC is selectively switched on only at the Co atoms and only at the Pt atoms. One can see that μ_{orb} at Co would indeed follow the trend of μ_{spin} if there was no SOC at the Pt atoms (cf. the left panel of Fig. 4 with the upper left panel of Fig. 1). It is the strong SOC at the Pt atoms which, via hybridization, affects μ_{orb} at the Co atoms and induces on them an *antiparallel* contribution to μ_{orb}. As the Pt concentration increases, so does the influence of SOC at Pt atoms. There is hardly any difference in μ_{orb} at Co if SOC is included on all Co atoms or if it is included only on that single Co atom for which μ_{orb} is calculated (cf. line with asterisks with line with crossed circles in the left panel of Fig. 4). This is a consequence of the fact that SOC at Co atoms is quite small and its off-site effects are, therefore, negligible.

As concerns μ_{orb} at Pt atoms, it follows from the right panel of Fig. 4 that the decisive contribution comes from the SOC at the Pt atoms. The contribution from the SOC at the Co atoms is very small (interestingly, it is antiparallel to μ_{spin}). If SOC is included only on a single Pt atom, μ_{orb} on that atom is by about 30% larger than if the SOC is included

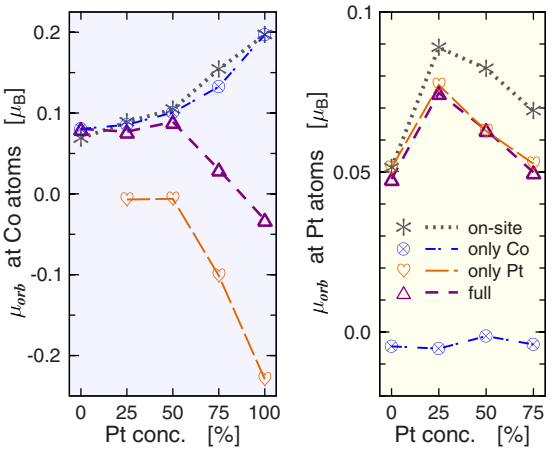

FIG. 4. (Color online) The orbital moments μ_{orb} at the Co atoms (left) and at the Pt atoms (right) in ordered Co-Pt systems calculated if SOC is included on a single atomic site only (dotted lines with asterisks), if SOC is included at all the atoms (short broken line with triangles), if SOC is included only at the Co atoms (chain line with crossed circles), and if SOC is included only at the Pt atoms (long broken line with hearts).

on all Pt atoms. Off-site SOC at Pt atoms thus generally suppresses μ_{orb} in Co-Pt systems.

One could see in Fig. 1 that μ_{orb} at Pt atoms follows approximately the trends of μ_{spin}. There are exceptions, however: For Co_3Pt, μ_{spin} at Pt atoms is smaller than for CoPt, while for μ_{orb} the situation is reversed. It is evident from Fig. 4 that this feature is not caused by off-site SOC contributions because the trends of μ_{orb} at Pt atoms with the composition do not depend on whether SOC is included on the on-site atom only or on all atoms. Rather, this effect has to be intrinsically connected with the electronic structure itself.

It is worth noting that μ_{orb} calculated if SOC is fully included is nearly equal to the sum of μ_{orb} calculated if SOC is considered only on Co atoms and only on Pt atoms (with an accuracy better than 5%). This additivity suggests that a first-order perturbation theory in fact can be applied to describe μ_{orb} in Co-Pt systems provided that off-site contributions are accounted for.[43]

As mentioned in Sec. III A, the simultaneous presence of the magnetization and SOC may lower the symmetry of the system. In particular, if $\boldsymbol{M}$ is parallel to [001], Co atoms in Co_3Pt and Pt atoms in $CoPt_3$ split into two groups. The spin magnetic moments of atoms of different groups are practically identical but the orbital magnetic moments differ. For Co_3Pt, Co atoms which are on planes where also Pt atoms are present have μ_{orb} that is about 30% smaller than Co atoms on planes which contain Co atoms only. For $CoPt_3$, the situation is somehow reversed: Pt atoms which are on planes which contain also Co atoms have μ_{orb} that is about 20% larger than Pt atoms on planes which contain solely Pt atoms. The decrease in μ_{orb} for Co atoms which are on planes where there are also Pt atoms can be understood intuitively: As follows from Fig. 4, Pt atoms have the general tendency to suppress μ_{orb} at neighboring Co atoms. As concerns the increase in μ_{orb} at Pt atoms, if they are mixed with Co atoms on one plane, one can assume that the decisive role is played

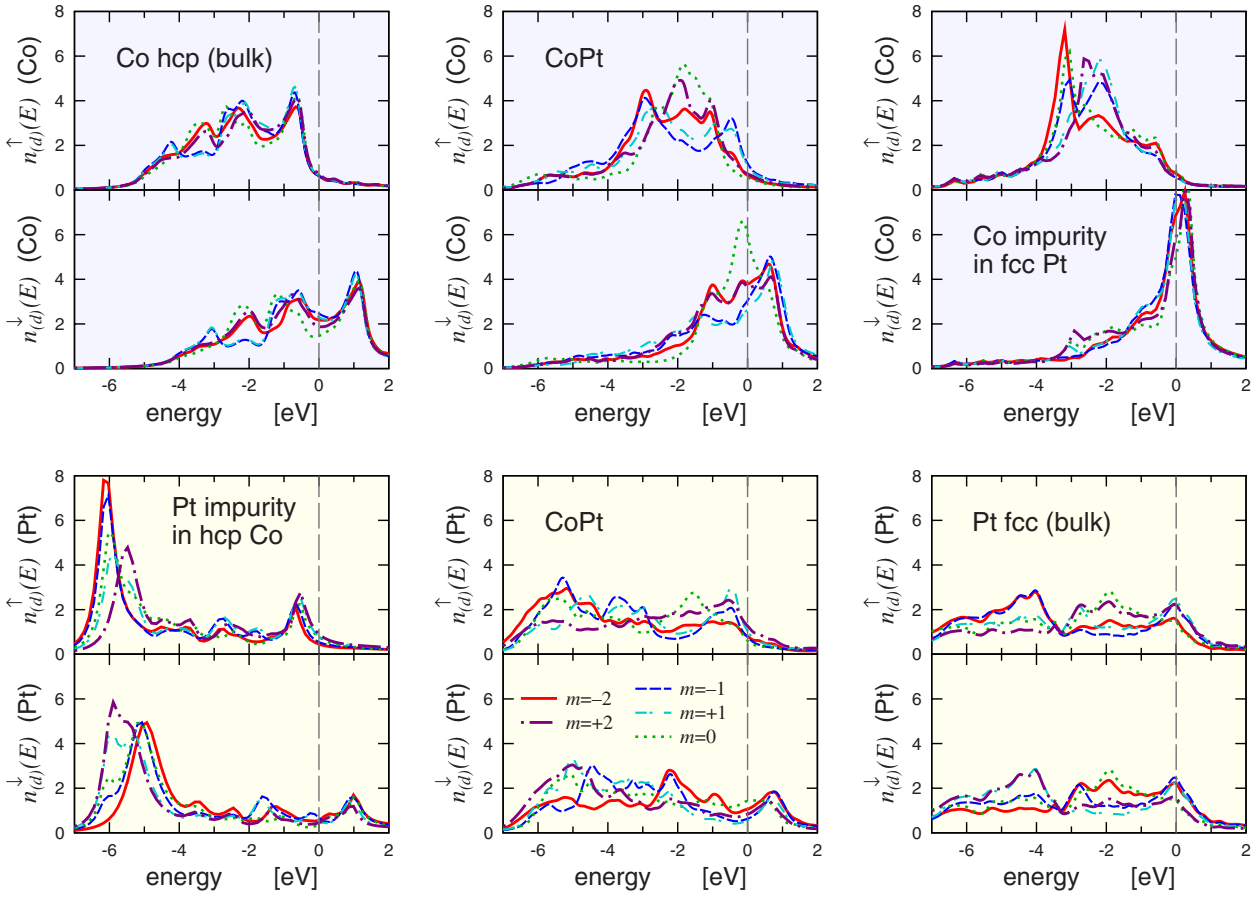

FIG. 5. (Color online) Spin-polarized d components of the local DOS at the Co (top) and Pt (bottom) atoms for selected ordered Co-Pt systems, resolved according to the magnetic quantum number m. Leftmost panels show data for elemental hcp Co and for a Pt impurity in Co, middle panels show data for CoPt, and rightmost panels show data for a Co impurity in Pt and for elemental fcc Pt. Data for $m=-2$ are shown as solid lines, for $m=+2$ as long chain lines, for $m=-1$ as broken lines, for $m=+1$ as short chain lines, and for $m=0$ as dots. The DOS is given in units of states/Ry.

by the Pt atoms themselves and that by mixing them with Co atoms, one effectively reduces the quenching of μ_{orb}.

Our finding that the SOC on Pt atoms significantly affects μ_{orb} at Co atoms can be seen to be analogous to an earlier finding that SOC on Au crucially affects μ_{orb} on V in VAu_4.[60] A similar situation arises also with the magneto-optical Kerr rotation angle θ_K: It was found for FePt that θ_K significantly changes if the SOC at Pt atoms is manipulated, while it varies only mildly if the SOC at Fe atoms is varied.[61]

Because of the presence of Pt atoms, the SOC cannot be considered a weak local perturbation in Co-Pt systems. Relation (3) between μ_{orb} and the spin polarization at E_F thus does not apply here [indeed, it will be shown in Sec. III D below that the difference $n^{\uparrow}(E_F)-n^{\downarrow}(E_F)$ is quite large for a Co impurity in Pt and yet μ_{orb} at Co is very small]. Likewise, the often-used Bruno formula connecting μ_{orb} to the magnetic anisotropy energy[62] will probably not work for systems with a high Pt content—as it was found not to be similarly valid at the Co/Au interface.[63]

D. Orbital-resolved densities of states

Figure 5 shows the density of the d states around Co and Pt atoms obtained for selected Co-Pt systems via LSDA calculations, resolved according to the magnetic quantum number m. The first thing we notice is that the localization of the DOS increases as the concentration of the given chemical type decreases. This is plausible: decreasing the concentration means decreasing the number of neighbors of its kind, reducing thus the hybridization and increasing the localization. Moreover, for Co atoms, the localization is stronger for the minority-spin states than for the majority-spin states. This is due to the fact that the Co minority-spin states do not have enough counterparts on the Pt atoms to hybridize with: The most prominent peak in the DOS of minority-spin states in pure hcp Co is 1 eV above E_F, which is an energy regime where there are practically no states for bulk Pt. For similar reasons, the localization of the DOS at Pt atoms is the strongest at the lower edge of the $5d$ band. This is a consequence of the larger width of the $5d$ band of pure Pt in comparison with the $3d$ band of Co: The states located about 5–6 eV below E_F have no counterparts at the Co atoms; thus if the Pt concentration decreases, so does the ability of these states to hybridize.

By inspecting individual m-resolved DOS curves, one finds that the most localized states are those with $m=0$ and the least localized those with $m=\pm 1$. The differences are, however, not big. Concerning the connection with μ_{orb}, the

most important contributions are those for $m=\pm 2$ because our calculations suggest that about 75% of the value of μ_{orb} stems from these states. This portion is nearly the same for all the Co-Pt systems, at both the Co and the Pt atoms. A similar observation was made earlier by Solovyev *et al.*[43] for CoPt and by Iwashita *et al.*[64] for $CoPt_3$.

The SOC is significantly stronger for Pt than for Co (we found that the SOC parameter ξ of the d states[65] is about 720 meV for the Pt atoms and 85 meV for the Co atoms along the whole Co-Pt series). It is thus not surprising that the difference between the DOSs for states with $m=+|m|$ and $m=-|m|$ is larger for Pt than for Co. Consistently with this, the difference between the DOSs for $+|m|$ and $-|m|$ is largest for systems with high Pt concentration and least for systems with low Pt concentration. Note that if the SOC is neglected altogether, the states differing by only the sign of m are degenerate.

For Co atoms, the splitting between the $\pm|m|$ states is more pronounced for the majority-spin states than for the minority-spin states. This can be understood in term of hybridization: The majority-spin Co states are more hybridized with Pt states than states with the minority spin and, therefore, they acquire a larger $\pm|m|$ splitting through this hybridization. It is worth noting that despite this, the majority-spin Co states contribute only negligibly to μ_{orb} at Co because they are almost filled and the contribution from the $+|m|$ states is counterbalanced by the contribution from the $-|m|$ states. For Pt atoms, on the other hand, there are nonnegligible contributions to μ_{orb} from both spin orientations: The total μ_{orb} of about $0.05\mu_B$ results from a positive contribution from the minority-spin states (typically about $0.20\mu_B$) and a negative contribution from the majority-spin states (typically about $0.15\mu_B$ for Co-Pt systems). Obviously, both contributions cancel exactly for pure nonmagnetic bulk Pt (their magnitude is about $0.24\mu_B$).

E. Influence of disorder

Results of our LSDA calculations for disordered Co-Pt alloys and for semiordered Co-Pt systems with the LRO parameter $S=0.6$ are shown in Fig. 6, together with the data for ordered systems. The data for fully ordered and for fully disordered systems were obtained in the FP mode; the data for semiordered systems were obtained using ASA. For the fully disordered systems, we performed the calculations both in the FP mode and in the ASA mode and found no significant differences. Relying on ASA results for the semiordered systems is thus reasonable.

Intuitively, introducing disorder should affect magnetism at Co atoms in two opposite ways. First, disorder leads to an increase in the *average* number of Co neighbors (Table I), increasing thereby the hybridization and decreasing μ_{spin}. Second, disorder itself introduces the occurrence of isolated Co atoms and clusters, which decreases the hybridization and increases μ_{spin}. The results presented in Fig. 6 indicate that disorder increases μ_{spin} at the Co atoms (and decreases μ_{spin} at the Pt atoms). This suggests that the effect of clustering prevails, even if it is incorporated only implicitly via the mean-field-type CPA.

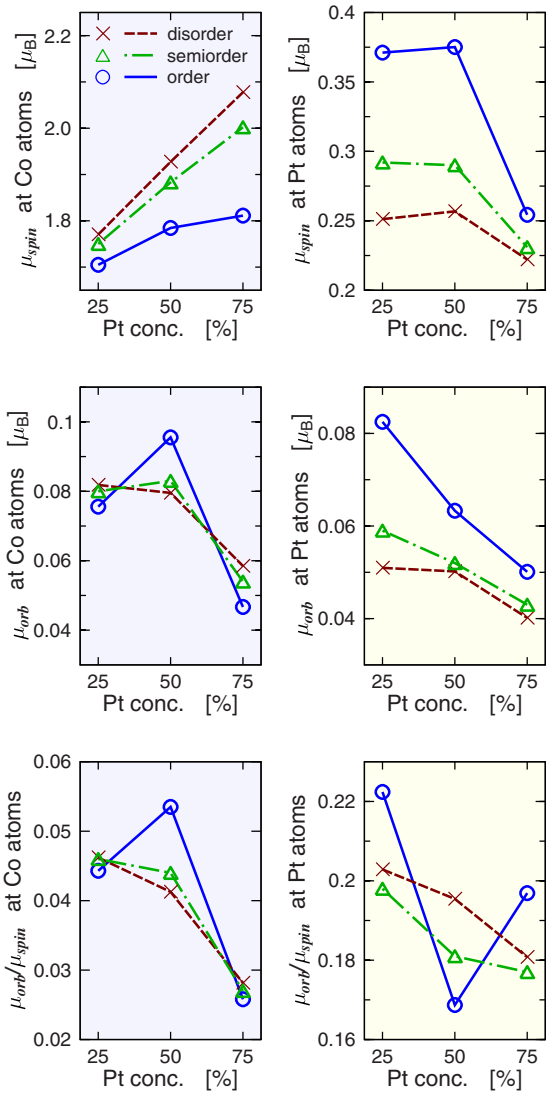

FIG. 6. (Color online) Magnetic moments μ_{spin} (top) and μ_{orb} (middle) and their ratio $\mu_{\mathrm{orb}}/\mu_{\mathrm{spin}}$ (bottom) for Co (left) and Pt atoms (right) in $Co_{1-x}Pt_x$ alloys in a fully ordered phase ($S=1.0$, solid lines with circles), in a semiordered phase ($S=0.6$, chain lines with triangles), and in a disordered phase ($S=0.0$, broken lines with crosses).

As concerns the Pt atoms, the dominant source of their magnetism is their hybridization with Co neighbors. Disorder decreases the average number of Co neighbors of Pt atoms (Table II) and therefore it decreases μ_{spin} at Pt atoms as well.

The orbital moment μ_{orb} at Co atoms is sometimes increased by the disorder (Co_3Pt and $CoPt_3$) and sometimes it is decreased (CoPt). The changes are, however, not big. For Pt atoms, disorder always decreases μ_{orb}. This decrease is sometimes relatively large (for Co_3Pt, it is by 50%) but it is always small in absolute magnitude (for Co_3Pt, μ_{orb} decreases from $0.083\mu_B$ to $0.051\mu_B$).

The changes in the ratio $\mu_{\mathrm{orb}}/\mu_{\mathrm{spin}}$ invoked by going from the ordered to the disordered phase are up to 20%. So if experiments are made on systems where the exact degree of

ordering is not known, this is the accuracy with which the μ_{orb}/μ_{spin} ratio can be evaluated (e.g., via XMCD).

In order to see how the magnetism of disordered Co-Pt alloys might be influenced by effects beyond the LSDA, another set of calculations for disordered and semiordered systems was performed but now with the Brooks OP term included (cf. Sec. III B). We found that for Co atoms, the OP scheme of Brooks leads to a more or less uniform enhancement of μ_{orb} by about $0.07\mu_B$, similar to the case of ordered systems. For Pt atoms, the changes in μ_{orb} were much smaller—again, similar to the ordered phase. This suggests that many-body effects will have similar consequences in the disordered Co-Pt compounds as in the ordered ones.

Results for semiordered systems lie somewhere between the results for the fully ordered systems and for the disordered systems, as expected. The only exception is the μ_{orb}/μ_{spin} ratio at Pt atoms in Co_3Pt and $CoPt_3$, but in these cases the values for disordered and semiordered phases are very close to each other anyway.

Let us return now to Table V, which compares $\mu_{orb}^{(d)}/\mu_{spin}^{(d)}$ calculated for ordered CoPt compound with experimental data which were in fact, however, obtained for a semiordered CoPt film,[23] with the LRO parameter $S=0.6$. It follows from our calculations that if pure LSDA is employed, the $\mu_{orb}^{(d)}/\mu_{spin}^{(d)}$ ratio for semiordered CoPt differs from the value for ordered CoPt by 18% for Co atoms and by 3% for Pt atoms. If the OP scheme of Brooks is employed, this difference is 13% for Co atoms and 1% for Pt atoms. The ratio $\mu_{orb}^{(d)}/\mu_{spin}^{(d)}$ is thus affected by the incomplete ordering of the sample but not so much as to invalidate the conclusions drawn from Table V. (One has to bear in mind that the results on the CoPt film obtained by Grange *et al.*[23] could have been affected by other effects such as Pt segregation.)

The theoretical spin moment μ_{spin} we obtained can be compared with the results of Paudyal *et al.*,[7] who calculated μ_{spin} of the $Co_{1-x}Pt_x$ series by: (i) using a nonrelativistic CPA scheme and (ii) using an augmented space recursion (ASR) method. Somewhat surprisingly, results of CPA calculations of Paudyal *et al.*[7] and of ours differ—especially for high Pt concentrations. E.g., the increase in μ_{spin} at Co atoms with increasing Pt concentration is steeper in our Fig. 6 than in the work of Paudyal *et al.*[7] (by about 50%). There are differences for Pt atoms as well: Our CPA calculations yield μ_{spin} at Pt atoms systematically by about $0.1\mu_B$ smaller than the CPA calculations of Paudyal *et al.*[7] (i.e., again by about 50%). The reason is unclear; we checked that relativistic effects are not responsible for this difference. For the ordered systems, on the other hand, our results and the results of Paudyal *et al.*[7] are very similar.

The differences between the two CPA calculations are larger than one would expect yet they are still "quantitative." A more essential difference emerges if one compares results of the CPA calculations with the results of the ASR calculation. For CoPt and $CoPt_3$, the CPA calculations (both of ours and of Paudyal *et al.*[7]) predict an *increase* in μ_{spin} at Co atoms if disorder is introduced, while the ASR calculation[7] predicts a *decrease* in μ_{spin}. This might indicate that magnetism of disordered $Co_{1-x}Pt_x$ alloys is significantly influenced by local random environment effects (fluctuations), which could be accounted for by the ASR technique[66] but which are neglected within the mean-field CPA approach. At the same time, the influence of various "technical factors" (such as, e.g., the approximate treatment of the self-consistency in the Coulomb potential in the ASR calculation) cannot be ruled out.

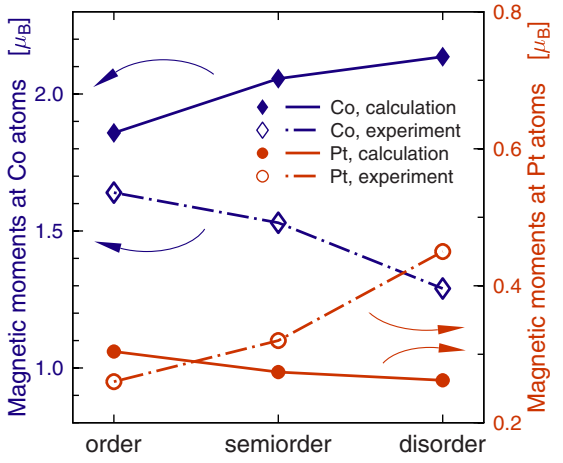

FIG. 7. (Color online) Total (spin plus orbital) magnetic moments at Co atoms (lines with diamonds, labeling on the left vertical axis) and at Pt atoms (lines with circles, labeling on the right vertical axis) for $CoPt_3$ with varying degrees of long-range order. Solid lines with full markers stand for our theoretical results; chain lines with open markers stand for the experimental results (Ref. 16).

For CoPt, another comparison is possible with the relativistic calculations of Uba *et al.*,[67] who simulated the disorder by a large supercell with a randomly generated distribution of Co and Pt atoms. Such a calculation includes the local environment effects but, on the other hand, the impact of disorder itself may be underestimated. The results of Uba *et al.*[67] suggest that disorder should increase μ_{spin} of Co atoms and decrease μ_{spin} of Pt atoms, in agreement with our results. However, the magnitudes of the changes are smaller in the study of Uba *et al.*[67] than in our work—especially for the Co atoms. As concerns μ_{orb}, there is again a partial agreement: Uba *et al.*[67] predicted that disorder should decrease μ_{orb} of Co atoms (similarly as in our study), while μ_{orb} of Pt atoms remains unchanged (in our study, it decreases).

Theoretical predictions concerning the influence of the disorder on local magnetic moments can be compared with the experiment of Menzinger and Paoletti,[16] who analyzed neutron-diffraction data for ordered, semiordered ($S=0.6$), and disordered $CoPt_3$. As follows from Fig. 7, there is a clear discrepancy between our calculations and the experiment in this case: the trends are quite opposite. One has to bear in mind, however, that assigning magnetic moments to different atomic types was by no means straightforward in the experiment of Menzinger and Paoletti[16]—certain assumptions about the magnetic form factors had to be made. If one deals with average magnetic moments per atom (obtained by direct magnetization measurements),[16] theory and experiment show similar trends (Table VII). It would certainly be interesting if more chemically selective experiments, such as XMCD, were available for $CoPt_3$ for various degrees of LRO.

To conclude this section, we would like to stress that the disagreements and controversies mentioned above concern

TABLE VII. Total (spin plus orbital) magnetic moments per atom of $CoPt_3$ provided by our calculations and by the magnetization measurements of Menzinger and Paoletti (Ref. 16) for varying degrees of long-range order. The unit is μ_B.

	S	Theor.	Expt.
Ordered	1.0	0.693	0.61
Semiordered	0.6	0.719	0.625
Disordered	0.0	0.731	0.66

TABLE VIII. Total magnetic moments per atom for ordered and disordered Co-Pt systems provided by the LSDA calculations and by experiment (Ref. 19). The unit is μ_B.

	Ordered		Disordered	
	Theor.	Expt.	Theor.	Expt.
Co_3Pt	1.449		1.465	1.46
CoPt	1.159	1.20	1.157	1.13
$CoPt_3$	0.693	0.67	0.731	0.70

only the *local* magnetic moments. When comparing total magnetic moments per atom (i.e., a quantity that can be measured directly), there is very good agreement between our calculations and the experiment for ordered as well as disordered systems (see Table VIII).

IV. CONCLUSIONS

Systematic trends of the spin and orbital magnetic moments in the Co-Pt systems with their composition can be identified. These trends are different for Co and for Pt atoms, yet they can be intuitively understood in terms of hybridization and site-dependent SOC. The value of μ_{orb} at Co atoms is strongly influenced by the SOC at the Pt atoms. Going beyond the LSDA significantly enhances μ_{orb} at Co atoms; for Pt atoms, the effect is not so big. The OP scheme of Brooks is efficient in remedying the LSDA deficiencies for low Pt concentration but it fails to do so for high Pt content. The LSDA+DMFT scheme allows to accurately reproduce the ratio of μ_{orb} to μ_{spin} at Co atoms over the whole concentration range. For Pt atoms, employing the LSDA+DMFT does not lead to a significant systematic change in μ_{orb} with respect to LSDA calculations. Some discrepancies between the calculated $\mu_{\mathrm{orb}}^{(d)}/\mu_{\mathrm{spin}}^{(d)}$ and between the ratio inferred from the Pt $L_{2,3}$ edge XMCD experiments remain.

Disorder as described by the CPA mean-field approach leads to an enhancement of μ_{spin} at the Co atoms and to a suppression of μ_{spin} at the Pt atoms. The orbital moment μ_{orb} at Co atoms does not exhibit big systematic changes if disorder is introduced. On the other hand, μ_{orb} at Pt atoms decreases with increasing disorder for all Pt concentrations. The $\mu_{\mathrm{orb}}/\mu_{\mathrm{spin}}$ ratio is, nevertheless, not significantly affected by the disorder. Data acquired by analyzing neutron-diffraction experiments disagree with our calculations concerning the effect of disorder on local magnetic moments at Co and Pt atoms in $CoPt_3$—even though there is agreement in the magnetic moments of whole unit cells.

ACKNOWLEDGMENTS

This work was supported by the Grant Agency of the Czech Republic under Project No. 202/08/0106, by the German Bundesministerium für Bildung und Forschung (BMBF) under Contract No. FKZ-05-KS1WMB/1, and by the Deutsche Forschungsgemeinschaft (DFG) under Priority Programs No. SPP 1153 and No. SPP 1136. The research in the Institute of Physics AS CR was supported by Project No. AV0Z-10100521 from the Academy of Sciences of the Czech Republic. Support by Project No. D 5-CZ 23/08-09 within the PPP program of DAAD and AS CR is also acknowledged. The authors are grateful to W. Grange for communications concerning his experiments and to V. Pierron-Bohnes for sending them the results contained in the thesis of C. E. Dahmani.

*sipr@fzu.cz; http://www.fzu.cz/~sipr

†hubert.ebert@cup.uni-muenchen.de; http://olymp.phys.chemie.uni-muenchen.de/ak/ebert/index_eng.html

[1] A. Kootte, C. Haas, and R. A. de Groot, J. Phys.: Condens. Matter **3**, 1133 (1991).

[2] M. Kim, A. J. Freeman, and R. Wu, Phys. Rev. B **59**, 9432 (1999).

[3] A. Kashyap, K. B. Garg, A. K. Solanki, T. Nautiyal, and S. Auluck, Phys. Rev. B **60**, 2262 (1999).

[4] V. N. Antonov, B. N. Harmon, and A. N. Yaresko, Phys. Rev. B **64**, 024402 (2001).

[5] I. Galanakis, M. Alouani, and H. Dreyssé, Phys. Rev. B **62**, 6475 (2000).

[6] I. Galanakis, M. Alouani, and H. Dreyssé, J. Magn. Magn. Mater. **242-245**, 27 (2002).

[7] D. Paudyal, T. Saha-Dasgupta, and A. Mookerjee, J. Phys.: Condens. Matter **16**, 2317 (2004).

[8] G. H. O. Daalderop, P. J. Kelly, and M. F. H. Schuurmans, Phys. Rev. B **44**, 12054 (1991).

[9] P. Ravindran, A. Kjekshus, H. Fjellvaag, P. James, L. Nordström, B. Johansson, and O. Eriksson, Phys. Rev. B **63**, 144409 (2001).

[10] I. V. Solovyev, Phys. Rev. Lett. **95**, 267205 (2005).

[11] A. B. Shick and O. N. Mryasov, Phys. Rev. B **67**, 172407 (2003).

[12] H. Ebert, B. Drittler, and H. Akai, J. Magn. Magn. Mater. **104-107**, 733 (1992).

[13] J. Minár and H. Ebert, Solid State Commun. **118**, 383 (2001).

[14] H. Ebert and H. Akai, Hyperfine Interact. **78**, 361 (1993).

[15] B. van Laar, J. Phys. (Paris) **25**, 600 (1964).

[16] F. Menzinger and A. Paoletti, Phys. Rev. **143**, 365 (1966).

[17] B. Antonini, F. Menzinger, and A. Paoletti, Phys. Lett. **25A**, 372 (1967).

[18] J. Crangle and W. R. Scott, J. Appl. Phys. **36**, 921 (1965).
[19] C. E. Dahmani, Ph.D. thesis, Louis Pasteur University, 1985.
[20] M. C. Cadeville and J. L. Morán-López, Phys. Rep. **153**, 331 (1987).
[21] R. J. Lange, S. J. Lee, D. W. Lynch, P. C. Canfield, B. N. Harmon, and S. Zollner, Phys. Rev. B **58**, 351 (1998).
[22] H. Maruyama, A. Urata, N. Kawamura, H. Yamazaki, E. K. Hlil, D. Raoux, S. Iwata, A. Rogalev, and J. Goulon, J. Electron Spectrosc. Relat. Phenom. **92**, 35 (1998).
[23] W. Grange, I. Galanakis, M. Alouani, M. Maret, J. P. Kappler, and A. Rogalev, Phys. Rev. B **62**, 1157 (2000).
[24] H. Maruyama, F. Matsuoka, K. Kobayashi, and H. Yamazaki, J. Magn. Magn. Mater. **140-144**, 43 (1995).
[25] W. Grange, M. Maret, J. P. Kappler, J. Vogel, A. Fontaine, F. Petroff, G. Krill, A. Rogalev, J. Goulon, M. Finazzi, and N. B. Brookes, Phys. Rev. B **58**, 6298 (1998).
[26] S. Imada, T. Muro, T. Shishidou, S. Suga, H. Maruyama, K. Kobayashi, H. Yamazaki, and T. Kanomata, Phys. Rev. B **59**, 8752 (1999).
[27] J. M. Cowley, Phys. Rev. **120**, 1648 (1960).
[28] D. M. S. Bagguley and J. A. Robertson, J. Phys. F: Met. Phys. **4**, 2282 (1974).
[29] S. S. A. Razee, J. B. Staunton, and F. J. Pinski, Phys. Rev. B **56**, 8082 (1997).
[30] S. H. Vosko, L. Wilk, and M. Nusair, Can. J. Phys. **58**, 1200 (1980).
[31] H. Ebert, in *Electronic Structure and Physical Properties of Solids*, Lecture Notes in Physics Vol. 535, edited by H. Dreyssé (Springer, Berlin, 2000), p. 191.
[32] R. Zeller, P. H. Dederichs, B. Újfalussy, L. Szunyogh, and P. Weinberger, Phys. Rev. B **52**, 8807 (1995).
[33] J. Minár, S. Bornemann, O. Šipr, S. Polesya, and H. Ebert, Appl. Phys. A: Mater. Sci. Process. **82**, 139 (2006).
[34] S. Bornemann, J. Minár, S. Polesya, S. Mankovsky, H. Ebert, and O. Šipr, Phase Transitions **78**, 701 (2005).
[35] T. Huhne, C. Zecha, H. Ebert, P. H. Dederichs, and R. Zeller, Phys. Rev. B **58**, 10236 (1998).
[36] M. S. S. Brooks, Physica B (Amsterdam) **130**, 6 (1985).
[37] J. Minár, L. Chioncel, A. Perlov, H. Ebert, M. I. Katsnelson, and A. I. Lichtenstein, Phys. Rev. B **72**, 045125 (2005).
[38] M. I. Katsnelson and A. I. Lichtenstein, Eur. Phys. J. B **30**, 9 (2002).
[39] L. V. Pourovskii, M. I. Katsnelson, and A. I. Lichtenstein, Phys. Rev. B **72**, 115106 (2005).
[40] S. Chadov, J. Minár, H. Ebert, A. Perlov, L. Chioncel, M. I. Katsnelson, and A. I. Lichtenstein, Phys. Rev. B **74**, 140411(R) (2006).
[41] J. Braun, J. Minár, H. Ebert, M. I. Katsnelson, and A. I. Lichtenstein, Phys. Rev. Lett. **97**, 227601 (2006).
[42] S. Chadov, J. Minár, M. I. Katsnelson, H. Ebert, D. Ködderitzsch, and A. I. Lichtenstein, Europhys. Lett. **82**, 37001 (2008).
[43] I. V. Solovyev, P. H. Dederichs, and I. Mertig, Phys. Rev. B **52**, 13419 (1995).
[44] P. M. Oppeneer, J. Magn. Magn. Mater. **188**, 275 (1998).
[45] R. Zeller, Modell. Simul. Mater. Sci. Eng. **1**, 553 (1993).
[46] M. M. Sigalas and D. A. Papaconstantopoulos, Phys. Rev. B **50**, 7255 (1994).
[47] S. Frota-Pessôa, Phys. Rev. B **69**, 104401 (2004).
[48] O. Šipr, S. Bornemann, J. Minár, S. Polesya, V. Popescu, A. Šimůnek, and H. Ebert, J. Phys.: Condens. Matter **19**, 096203 (2007).
[49] I. Cabria, B. Nonas, R. Zeller, and P. H. Dederichs, Phys. Rev. B **65**, 054414 (2002).
[50] W. D. Brewer, A. Scherz, C. Sorg, H. Wende, K. Baberschke, P. Bencok, and S. Frota-Pessoa, Phys. Rev. Lett. **93**, 077205 (2004).
[51] M. Sargolzaei, Ph.D. thesis, Technische Universität Dresden, 2006.
[52] H. P. Wijn, *Magnetic Properties of Metals: d-Elements, Alloys and Compounds*, (Springer, Berlin, 1991).
[53] G. G. Scott and H. W. Sturner, Phys. Rev. **184**, 490 (1969).
[54] O. Eriksson, B. Johansson, R. C. Albers, A. M. Boring, and M. S. S. Brooks, Phys. Rev. B **42**, 2707 (1990).
[55] B. T. Thole, P. Carra, F. Sette, and G. van der Laan, Phys. Rev. Lett. **68**, 1943 (1992).
[56] P. Carra, B. T. Thole, M. Altarelli, and X. Wang, Phys. Rev. Lett. **70**, 694 (1993).
[57] J. Vogel, A. Fontaine, V. Cros, F. Petroff, J. P. Kappler, G. Krill, A. Rogalev, and J. Goulon, Phys. Rev. B **55**, 3663 (1997).
[58] H. Ebert, R. Zeller, B. Drittler, and P. H. Dederichs, J. Appl. Phys. **67**, 4576 (1990).
[59] H. Ebert, J. Minár, and V. Popescu, in *Band-Ferromagnetism: Ground-State and Finite-Temperature Phenomena*, Lecture Notes in Physics Vol. 580, edited by W. N. K. Baberschke and M. Donath (Springer, Berlin, 2001), p. 371.
[60] I. Galanakis, P. M. Oppeneer, P. Ravindran, L. Nordström, P. James, M. Alouani, H. Dreysse, and O. Eriksson, Phys. Rev. B **63**, 172405 (2001).
[61] H. Ebert, H. Freyer, and M. Deng, Phys. Rev. B **56**, 9454 (1997).
[62] P. Bruno, Phys. Rev. B **39**, 865 (1989).
[63] C. Andersson, B. Sanyal, O. Eriksson, L. Nordström, O. Karis, D. Arvanitis, T. Konishi, E. Holub Krappe, and J. H. Dunn, Phys. Rev. Lett. **99**, 177207 (2007).
[64] K. Iwashita, T. Oguchi, and T. Jo, Phys. Rev. B **54**, 1159 (1996).
[65] J. W. Davenport, R. E. Watson, and M. Weinert, Phys. Rev. B **37**, 9985 (1988).
[66] T. Saha, I. Dasgupta, and A. Mookerjee, J. Phys.: Condens. Matter **8**, 1979 (1996).
[67] L. Uba, S. Uba, O. Horpynyuk, V. N. Antonov, and A. N. Yaresko, J. Appl. Phys. **91**, 775 (2002).